

# Aerobic Oxidation of Hydroxymethylfurfural and Furfural by Using Heterogeneous $\text{Co}_x\text{O}_y\text{-N@C}$ Catalysts

Jin Deng,<sup>[a]</sup> Hai-Jie Song,<sup>[a]</sup> Min-Shu Cui,<sup>[a, b]</sup> Yi-Ping Du,<sup>[a]</sup> and Yao Fu<sup>\*,[a]</sup>

2,5-Furandicarboxylic acid (FDCA) is considered to be a promising replacement for terephthalic acid since they share similar structures and properties. In contrast to FDCA, 2,5-furandicarboxylic acid methyl (FDCAM) has properties that allow it to be easily purified. In this work, we reported an oxidative esterification of 5-hydroxymethylfurfural (HMF) and furfural to prepare corresponding esters over  $\text{Co}_x\text{O}_y\text{-N@C}$  catalysts using  $\text{O}_2$  as benign oxidant. High yield and selectivity of FDCAM and

methyl 2-furoate were obtained under optimized conditions. Factors which influenced the product distribution were examined thoroughly. The  $\text{Co}_x\text{O}_y\text{-N@C}$  catalysts were recycled five times and no significant loss of activity was detected. Characterization of the catalysts could explain such phenomena. Using XPS and TGA, we made a thorough investigation of the effects of ligand and pyrolysis temperature on catalyst activity.

## Introduction

With the diminishing reserves of fossil resources and the increasing demand for petroleum-based chemicals, utilization of renewable replacements for petroleum-derived products has grown in popularity. Of particular appeal is biomass, which can be used as an alternative carbon source and is readily available worldwide.<sup>[1]</sup> 5-Hydroxymethylfurfural (HMF) can be obtained from biomass-based carbohydrates, and has the potential to be upgraded to several valuable compounds.<sup>[2]</sup> Via oxidation, HMF can be transformed to 2,5-furandicarboxylic acid (FDCA). FDCA is considered to be a promising replacement for terephthalic acid (TPA), which is used in large quantities for polymers and fine chemicals production.<sup>[3]</sup>


Various methods of heterogeneous catalysis have been studied for the oxidation of HMF to FDCA. Typically, supported noble metals such as Pd,<sup>[4]</sup> Pt,<sup>[5]</sup> Au,<sup>[6]</sup> Ru<sup>[7]</sup> and bimetallic catalysts<sup>[8]</sup> were utilized. Despite the increasing utilization of these metals, previous work on catalytic oxidation revealed a relatively wide variation in performance. Yields of FDCA ranging from 48% to nearly quantitative were achieved in different reaction systems. Considering the high cost of catalysts, a base metal, cobalt, was used to convert fructose into FDCA.<sup>[9]</sup> With a yield of 71%, FDCA was converted directly from fructose using  $\text{Co}(\text{acac})_3$  encapsulated in a sol-gel silica matrix as catalysts.

However, FDCA is a solid which has large polarity, no precise melting point or boiling point, and low solubility in most solvents. Conventional purification methods such as vacuum distillation and recrystallization have no feasibility on FDCA. Hence, regarding FDCA purification, there is still a dearth of straightforward and eco-friendly methods. A possible way to overcome this inconvenience is to produce the corresponding ester, 2,5-furandicarboxylic acid dimethyl ester (FDCDM), which can be easily purified through vacuum distillation and transformed to FDCA through a simple hydrolysis reaction. Moreover, instead of FDCA, FDCDM can be used directly to synthesize polymers through transesterification reaction. Christensen et al.<sup>[10]</sup> reported a method for HMF oxidative esterification using  $\text{Au/TiO}_2$  catalyst in MeOH with an addition of MeONa base. They obtained 60% yield of FDCDM under 4 bar  $\text{O}_2$  at 130 °C for 3 h. Furthermore, Corma et al.<sup>[11]</sup> reported the conversion of HMF to FDCDM over  $\text{Au/CeO}_2$  catalyst. The reaction was also performed in methanol and a yield of 99 mol% was achieved. Taking into consideration cost and ease of purification, a noble-metal-free approach for the oxidative esterification of HMF to FDCDM is worth exploring.

Recently, Beller et al.<sup>[12]</sup> have applied pyrolyzed molecularly defined complexes in catalytic oxidation and reduction of organic chemicals. Of most attractive is the application of cobalt-based catalysts in the direct conversion of benzylic alcohols to the corresponding methyl ester in methanol.<sup>[12b]</sup> As reported, the whole procedure consists of the following steps: first is the oxidation of alcohol to aldehyde; then in methanol, aldehyde converts to the corresponding hemiacetal; finally, via dehydrogenation, hemiacetal transforms to ester. Under 0.1 MPa oxygen at 80 °C for 24 h, the esterification of various benzylic alcohols and heterocyclic alcohols was performed over the cobalt catalysts in a good yield (85–97%). Furthermore, diesters and triesters were obtained directly with a yield up to 91%.

[a] Dr. J. Deng, H.-J. Song, M.-S. Cui, Y.-P. Du, Prof. Dr. Y. Fu  
Anhui Province Key Laboratory of Biomass Clean Energy  
Department of Chemistry  
University of Science and Technology of China  
Hefei 230026 (PR China)  
Fax: (+86)-551-6360-6689  
fuyao@ustc.edu.cn

[b] M.-S. Cui  
Nano Science and Technology Institute  
University of Science and Technology of China  
Suzhou 215123 (PR China)

 Supporting Information for this article is available on the WWW under <http://dx.doi.org/10.1002/cssc.201402843>.

Herein, we attempted to apply pyrolyzed  $\text{Co}_x\text{O}_y\text{-N@C}$  catalysts to the oxidative esterification of biomass-derived furans including furfural and HMF. As expected, good results were obtained on both chemicals. For furfural, full conversion and a 95% yield of methyl 2-furoate (MF) was obtained under 0.1 MPa  $\text{O}_2$  at 60 °C for 12 h. Furthermore, we achieved a 100% conversion of HMF and a 96% yield of target products at 100 °C under 1 MPa  $\text{O}_2$  for 6 h requiring an addition of K-OMS-2. Both reactions were performed in methanol over heterogeneous  $\text{Co}_x\text{O}_y\text{-N@C}$  catalysts with the aid of 0.2 equivalent amounts of  $\text{K}_2\text{CO}_3$ .

## Results and Discussion

To study the feasibility of the cobalt-based catalysts for the catalysis of biomass-derived compounds, we tested initially the catalytic esterification of furfural in  $\text{CH}_3\text{OH}$ . Gratifyingly, the  $\text{Co}_x\text{O}_y\text{-N@C}$  catalysts performed well in the reaction. Later, to investigate the optimum catalytic efficiency, exploratory experiments with different metals and ligands were performed under the same reaction conditions (Table 1, entries 1–3). For a 12 h reaction time, under 0.1 MPa  $\text{O}_2$  at 60 °C, Co with ligand 1,10-phenanthroline (1,10-phen) showed the best activity in comparison with Pd(1,10-phen) and Co with 2,2-dipyridine (2,2-

diPy) as ligand. This result is consistent with the work of Beller et al.<sup>[12d]</sup>

From the view of structure, difference between the two ligands is reflected in the connection of pyridines. In 2,2-diPy, a  $\sigma$ -bond acts as bridge, while in 1,10-phen a benzene ring acts as bridge. As a result, 2,2-diPy shows more flexibility which contributes to a difficulty in the formation of graphene-type layers by nitrogen ligand during the pyrolysis process. Previous work<sup>[13]</sup> concluded that in metal-N@C catalysts, active site mainly consists of pyridine-type nitrogen and graphene-type nitrogen. Therefore a lack of graphene-type nitrogen leads to a low catalytic activity. XPS data is shown in Figure 1. In the N1s spectra, distinct peaks with electron-binding energies of 403.6 eV and 400.8 eV have been observed and can be attributed to graphene-type nitrogen and pyrrole-type nitrogen, respectively. Peaks with binding energies of 399.6 eV and 398.4 eV represent pyridine-type nitrogen (bond with cobalt) and nitrogen of ligand (pyridine-type nitrogen) in  $\text{Co}_x\text{O}_y\text{-2,2-diPy/C}$  respectively.<sup>[14]</sup> And 399.7 eV and 398.6 eV are characterized as pyridine-type nitrogen and as nitrogen of ligand in  $\text{Co}_x\text{O}_y\text{-1,10-phen/C}$  respectively.<sup>[14]</sup> From the comparison of  $\text{Co}_x\text{O}_y\text{-2,2-diPy/C}$  with  $\text{Co}_x\text{O}_y\text{-1,10-phen/C}$  in Figure 1a), no indication of graphene-type nitrogen and a lower amount of pyridine-type nitrogen have been detected in  $\text{Co}_x\text{O}_y\text{-N@C}$  using 2,2-diPy as ligand. In addition, the chelate of  $\text{Co}(\text{OAc})_2\cdot 4\text{H}_2\text{O}$  and 2,2-diPy has a lower activation energy which contributes to easier cleavage and gasification (TGA data shown in Figure S8, Supporting Information). The loss of acetate reduces the amount of oxygen in the catalyst. As a result, under the same pyrolysis temperature, Co-2,2-diPy has less potential to form cobalt oxides, resulting in a low activity of Co-2,2-diPy catalysts. XPS data of  $\text{Co}2\text{p}^{3/2}$  for support of the conclusions is shown in Figure 1b. Peaks with binding energy of 785.6 eV to 786.6 eV, 781.0 eV, 779.3 eV to 780.0 eV, and 778.5 eV can be attributed to a satellite peak of cobalt, bonding of cobalt and nitrogen, bonding of cobalt and oxygen and  $\text{Co}^0$  respectively.<sup>[15]</sup> Obviously, the content of oxidized cobalt is higher in the

Table 1. Oxidative esterification of furfural to MF. <sup>[a]</sup>				
Entry	Metal <sup>[b]</sup>	Ligand	Conversion <sup>[c]</sup> [%]	Yield <sup>[c]</sup> [%]
1	Co	1,10-phen	100	95
2	Pd	1,10-phen	12	4
3	Co	2,2-diPy	58	46
4 <sup>[d]</sup>	Co	1,10-phen	54	42
5 <sup>[d]</sup>	Mn	1,10-phen	9	-
6 <sup>[d]</sup>	Pd	1,10-phen	15	1

[a] Conditions: 0.1 MPa  $\text{O}_2$ , 60 °C, 12 h, 0.2 equiv  $\text{K}_2\text{CO}_3$ . [b] Metal loading: 3%; 25 mg catalyst. [c] Determined by GC. [d] Reactant: furfuryl alcohol.

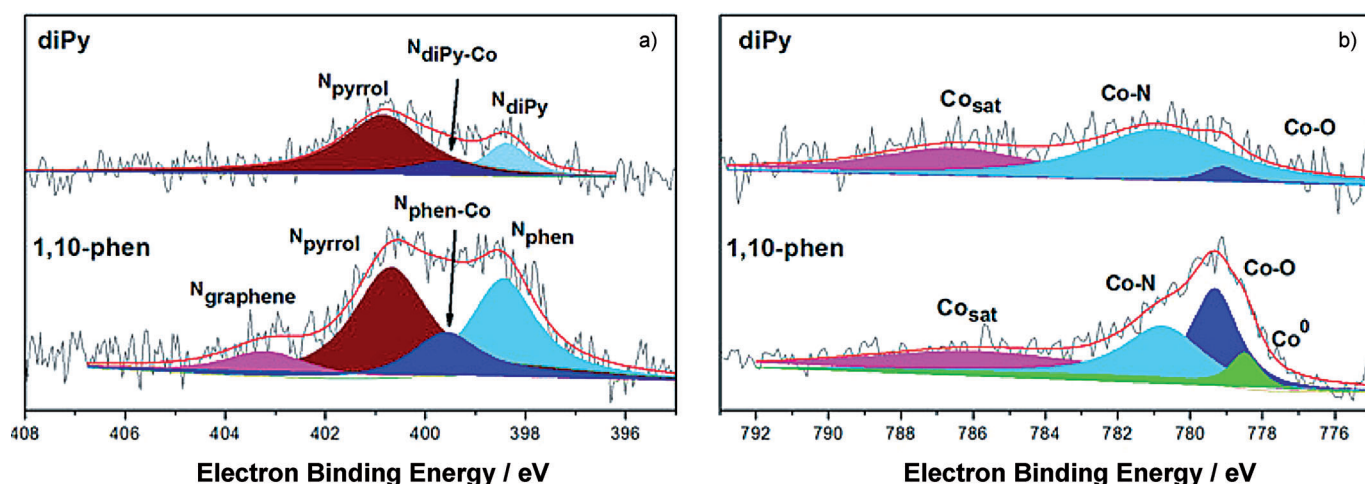


Figure 1. XPS of the a) N1s and b)  $\text{Co}2\text{p}^{3/2}$  for Co with ligands diPy and 1,10-phen.

pyrolyzed  $\text{Co}_x\text{O}_y\text{-N@C}$  using ligand 1,10-phen with a certain amount of  $\text{Co}^0$  present existence.

A similar result was observed in the oxidative esterification of furfuryl alcohol (FA) over the carbon-supported catalysts (Table 1, entries 4–6).  $\text{Co}(1,10\text{-phen})$  catalysts showed the best performance while  $\text{Mn}(1,10\text{-phen})$  did not show any activity toward ester formation, only a 5 % yield of furfural was obtained.

As expect, the cobalt-based carbon-supported catalysts were effective for the oxidation of HMF in methanol as well (Table 2). Under 0.1 MPa  $\text{O}_2$  at 60 °C for 12 h, we obtained a 95 % conversion of HMF and obtained FDCDM, 2,5-furandicarboxylic acid monomethyl ester (FDCMM), FDCA, and 5-hydroxymethyl-2-furoic acid methyl ester (HMFM) in 28 %, 30 %,

the aim of improving the conversion of HMFM, according to our previous work,<sup>[16]</sup> we introduced K-OMS-2, an efficient heterogeneous catalyst for HMF oxidation to DFF, into the HMF oxidative esterification reaction system. To our delight, the yield of HMFM declined to 2 % under the optimal conditions. Meanwhile, we obtained the highest yield of FDCAM of 95 %.

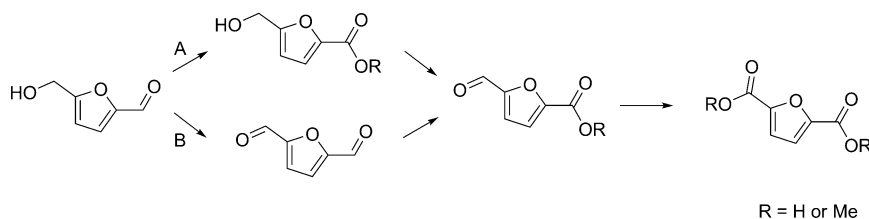
To study the influence of reaction conditions on the distribution of HMF oxidation products, a comprehensive investigation was performed. Variables including catalyst pyrolysis temperature, Co loading, amount of catalysts, alkaline intensity, reaction time, oxygen pressure, and reaction temperature were examined thoroughly.

### Catalyst activity

In order to explore how pyrolysis temperature affected the catalyst activity, we tested temperatures ranging from 200 °C to 1000 °C with a gradient of 200 (Figure 2). All the experiments were performed under 1 MPa  $\text{O}_2$  at 80 °C for 12 h over 25 mg 3wt %  $\text{Co}_x\text{O}_y\text{-N@C}$  with an equal amount of K-OMS-2. As shown in the figure, catalysts pyrolyzed at 200 °C exhibited little activity toward FDCAM formation, even though a 95 % conversion of

HMF was obtained. The main product was DFF categorized in the series "others". Along with the increase of pyrolysis tem-

1 %, and 36 % yield, respectively. Given the situation that the major product was HMFM, a change of reaction condition was made in an effort to improve the yield of 2,5-furandicarboxylic acid methyl (FDCAM, which corresponds to the sum of FDCDM, FDCMM, and FDCA). With an increase in  $\text{O}_2$  pressure and reaction temperature, the yield of FDCDM had been greatly improved while a decrease of HMFM was clearly detected. The optimized conditions, 1 MPa  $\text{O}_2$  and 100 °C, led to FDCDM, FDCMM, FDCA, and HMFM in 38 %, 44 %, 1 %, and 12 % yield respectively. Taking the result of the oxidative reaction of FA into account, we deduced that the rate-determining step was the alcohol oxidation to aldehyde. Typically, there are two pathways for HMF to FDCDM (Scheme 1). One is through aldehyde oxidation to HMFM (path A), the other is through alcohol oxidation to 2,5-diformylfuran (DFF, path B). Under the same mild reaction conditions with furfural, we examined the catalytic efficiency for DFF. The yield of FDCDM, FDCMM, FDCA, and HMFM was 53 %, 46 %, 0 and 1 %, respectively. Hence, with



**Scheme 1.** Possible pathways of HMF transformation.

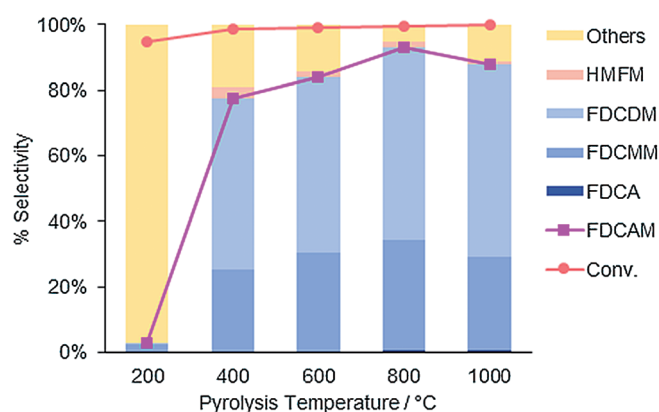


**Figure 2.** Effects of pyrolysis temperature on catalyst activity.

perature, catalytic activity was significantly improved. The carbon-supported catalysts that were pyrolyzed at 800 °C led to the best performance of 93 % yield of FDCAM. For 1000 °C pyrolysis temperature, the activity declined slightly. Thus, 800 °C

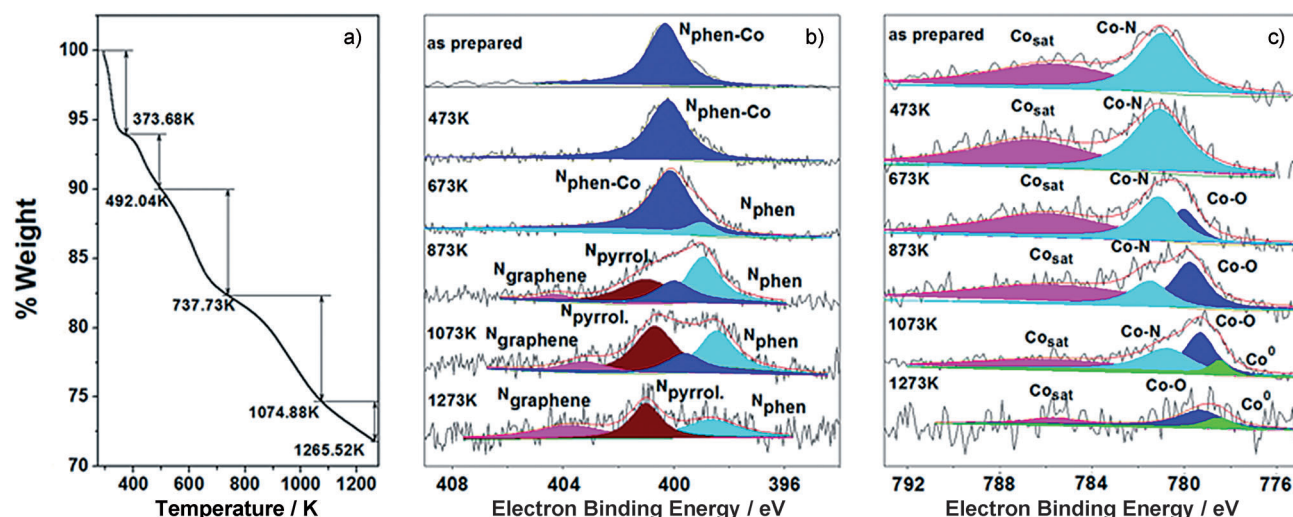


**Figure 3.** a) TGA data of nonpyrolyzed Co<sub>x</sub>O<sub>y</sub>-N@C; b) XPS of the N1s and c) Co2p<sub>3/2</sub> for Co<sub>x</sub>O<sub>y</sub>-N@C prepared at different pyrolysis temperature.

was chosen to be the optimal pyrolysis temperature in the following study.

To elucidate the effect of pyrolysis temperature on catalytic activity, we performed detailed investigation using thermogravimetric analysis (TGA) and X-ray photoelectron spectroscopy (XPS). Result of TGA tests for nonpyrolyzed Co<sub>x</sub>O<sub>y</sub>-N@C catalysts are shown in Figure 3a). The Figure reveals the following information:<sup>[17]</sup> 1) Below 100 °C, the loss of weight is mainly due to the loss of crystal water. 2) From 100 °C to 200 °C, acetate begins to change. Therefore, catalysts pyrolyzed at 200 °C show little activity on HMF esterification. 3) Over 200 °C, continued rise of temperature brings about a cleavage of Co(1,10-phen) to free 1,10-phen and cobalt, leading to a formation of cobalt oxides from the free cobalt and oxygen. In this way, the catalysts adopt the active state. This is consistent with the experimental results. A significant difference of FDCAM yield was obtained between pyrolysis temperature 200 °C and 400 °C. 4) In the range of 400 °C to 800 °C, further conversion of 1,10-phen results in the formation of pyrrole-type nitrogen and graphene-type layers. Thus, the most active catalysts can be obtained. In the experiment data, catalysts pyrolyzed at 800 °C showed the best performance. 5) More than 800 °C, Co<sub>x</sub>O<sub>y</sub>-N@C catalysts begin to decompose.

Corresponding results analyzed by XPS are shown in Figure 3b) and c). In the N1s spectra, four distinct peaks with electron binding energy of 403.6 eV, 400.8 eV, 399.7 eV, and 398.6 eV were detected and can be attributed to graphene-type nitrogen, pyrrole-type nitrogen, pyridine-type nitrogen (bonded with cobalt), and nitrogen of 1,10-phen (pyridine-type nitrogen), respectively.<sup>[14]</sup> For the Co2p<sub>3/2</sub> spectra, peaks with electron binding energy of 785.6 eV to 786.6 eV, 781.0 eV, 779.3–780.0 eV, and 778.5 eV can be attributed to Co satellite, Co–N, Co–O, and Co<sup>0</sup>.<sup>[15]</sup> Below 200 °C, only the peak of Co(1,10-phen) is observed. There is an emergence of pyridine-type nitrogen and Co–O at pyrolysis temperatures of over 400 °C. Along with the increase of temperature, from 600 °C, sustaining cleavage of Co(1,10-phen) results in the formation

of pyrrole-type nitrogen and graphene-type nitrogen as well as the acceleration of pyridine-type nitrogen and cobalt oxides. From 800 °C, the appearance of Co<sup>0</sup> is detected due to the reducibility of carbon. At a pyrolysis temperature of 1000 °C, as shown in the spectra, interaction between Co and 1,10-phen no longer exists and the whole catalyst begins to decompose. Thus, the catalyst with the highest activity can be obtained through a pyrolysis process at 800 °C. Additionally, changes in satellite peaks of Co illustrate that, in Co<sub>x</sub>O<sub>y</sub>-N@C catalysts, the amounts of Co<sup>2+</sup> are variable.

Characterization by energy-dispersive X-ray spectroscopy elemental mapping (EDS) also confirms the existence of cobalt oxides. As shown in Figure S7, Supporting Information, in the combined image, the area in which cobalt is present is also abundant in oxygen while the amount of carbon is low.

Similar results can be summed up from previous works.<sup>[18]</sup> Generally, in inert atmosphere, Co–N@C catalysts pyrolyzed at 600 °C to 800 °C has the best catalytic activity. In this range, the metal–nitrogen chelating structures as catalytic active sites are uniformly dispersed on the carbon support. Above 800 °C, metal–nitrogen chelating bond would break, resulting in a decline of catalytic activity. Two possible explanations for this phenomenon have been raised as follows: 1) high temperatures favor the generation of inert particles of metals, metal oxides, or metal carbides;<sup>[19]</sup> 2) as the metal–nitrogen bond breaks, the density of active sites distributing on the surface of catalyst also decreases.<sup>[20]</sup> Another view point states that, of the two active sites, pyridine-type nitrogen and graphene-type nitrogen, the former one is more active. With the increase of pyrolysis temperature, amounts of graphene-type nitrogen will increase with a drop in the amount of pyridine-type nitrogen.<sup>[13]</sup> Thus, above the optimal pyrolysis temperature, the catalytic activity will decrease.

Furthermore, reactions were also conducted to probe the effects of Co loading and catalyst amount on the catalytic efficiency. Typically, we used 3 wt% Co with 1,10-phen ligand adsorbed on active carbon and pyrolyzed at 800 °C for 2 h. All re-



actions were performed over 25 mg  $\text{Co}_x\text{O}_y\text{-N@C}$  catalysts and 25 mg K-OMS-2. Both decreasing the Co loading to 1% or increasing it to 5% led to a drop of FDCAM yield. The yield declined from 96% to 43% and 87% respectively. Similarly, reducing the amount of catalysts to 10 mg afforded a decline of FDCAM from 96% to 82%. Similar results of metal loading effect have been discussed in previous literature.<sup>[21]</sup> Over-loading metal may lead to the formation of particles with no activity. And the inactive metals, metal oxides, and metal carbides hinder the reactants entering the pores of carbon support. Hence, no effective interaction between reactants and active sites leads to a loss of catalytic activity.<sup>[22]</sup> Brunauer–Emmett–Teller (BET) data of 3% and 5%  $\text{Co}_x\text{O}_y\text{-N@C}$  is listed in ESI. Results show a significant loss of BET surface area and pore volume with an increase of average pore diameter when Co loading increases from 3% to 5%.

### Effects of reaction conditions

As shown in Figure 4, we examined the influence of oxygen pressure on the reaction yield. All the data were collected at 60 °C for a 12 h reaction time over 25 mg  $\text{Co}_x\text{O}_y\text{-N@C}$  and K-OMS-2. Initially, as in the oxidation of furfural, reaction pressure

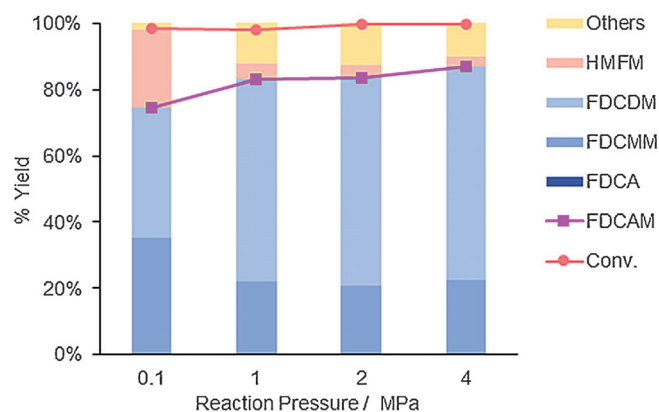


Figure 4. Product distribution under different reaction pressures.

was set as 0.1 MPa, and a 75% yield of FDCAM was obtained. For the purpose of getting better results, oxygen pressure was expanded to 1 MPa, 2 MPa, and 4 MPa separately. As expected, the yield of FDCAM increased gradually when the pressure was increased. Due to an increase of only 4% yield of FDCAM when pressure was increased from 1 MPa to 4 MPa, we chose 1 MPa as the most cost-effective oxygen pressure.

Studies on reaction temperature were conducted at 60 °C, 80 °C, 100 °C, and 120 °C under 1 MPa  $\text{O}_2$  for 12 h (Figure 5). Within the range of 60 °C to 100 °C, a continuous growth of FDCAM yield and drop of FDCDM yield were observed concurrently. One reason for the growth was that the conversion of DFF (categorized in the series “others”) to FDCAM improved with increasing the reaction temperature. The drop was due to the accelerated hydrolysis of FDCDM. The highest yield of 95% was obtained at 100 °C, composed of 50% FDCDM, 45%

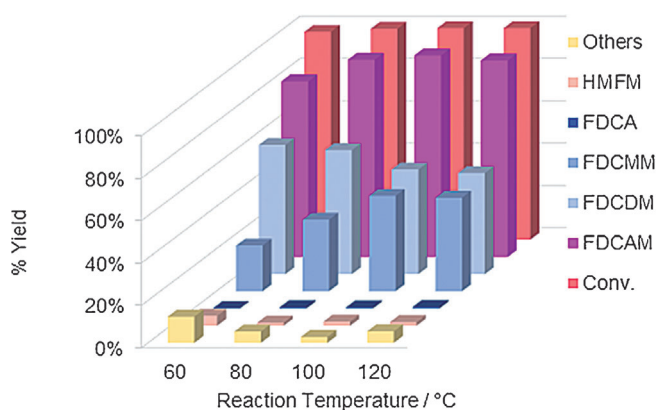


Figure 5. Product distribution under different reaction temperatures.

FDCMM, and less than 1% FDCA. In the range of 100 °C to 120 °C, yield of FDCAM fell to 93%. This might be due to a further decomposition of FDCMM and FDCDM.

In the oxidative esterification of furfural, a 12 h reaction time afforded the best result. Because we increased the reaction pressure and temperature, a series experiments were performed to verify the effects on reaction rate acceleration. Reaction time 1 h, 2 h, 4 h, 6 h, and 12 h were tested separately under 1 MPa  $\text{O}_2$  at 100 °C (Figure 6). Gratifyingly, a reaction time of 6 h achieved the best performance of 96% yield of FDCAM.

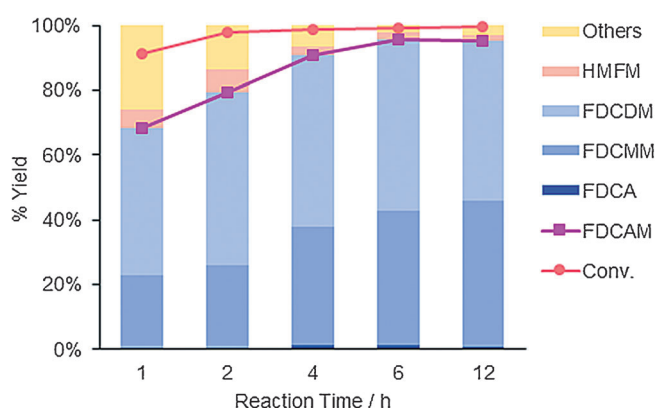


Figure 6. Product distribution under different reaction times.

### Effects of alkaline intensity

Despite all the factors discussed above, alkaline intensity was another essential element in the oxidative esterification of HMF (Table 3). Starting with  $\text{K}_2\text{CO}_3$ , salts with different alkaline were tested under the optimal reaction conditions. Along with the reduction of alkaline, a drop of FDCAM yield was clearly detected. The possible intermediates of oxidative esterification of HMF, aldehyde and hemiacetal, indicated an elimination of the  $\alpha\text{-H}$  of the hydroxyl. On the other hand, the presence of alkali was conducive to the occurrence of dehydrogenation.

**Table 3.** Effects of alkaline intensity on the esterification of HMF.<sup>[a]</sup>

Entry	Base <sup>[b]</sup>	Conversion <sup>[c]</sup> [%]	Yield <sup>[c]</sup> [%]				
			HMFM	FDCDM	FDCMM	FDCA	FDCAM
1	K <sub>2</sub> CO <sub>3</sub>	99	2	53	42	1	96
2	Na <sub>2</sub> CO <sub>3</sub>	> 99	0	58	39	1	98
3	KHCO <sub>3</sub>	> 99	1	68	20	0	88
4	NaOAc	91	4	61	3	0	64
5	Na <sub>2</sub> HPO <sub>4</sub>	70	3	42	2	0	44

[a] Conditions: 1 MPa O<sub>2</sub>, 100 °C, 6 h, 25 mg Co<sub>x</sub>O<sub>y</sub>-N@C-800 and 25 mg K-OMS-2. [b] 0.2 Equiv. [c] Determined by HPLC.

### Effects on product distribution

Our original intention was to explore a method for direct conversion of HMF to FDCDM, and then obtain FDCA through purification and hydrolysis. However, the target product was appearing in three forms because the FDCDM hydrolyzed. There are two reasons for this: Both the alkaline reaction base and the increase of reaction temperature accelerated the hydrolysis process. As shown in Figure 3 and Table 3, with the increase of alkaline and temperature, the proportion of FDCMM and FDCA increased continuously while an apparent decline in the proportion of FDCDM was observed.

Furthermore, considering the byproduct was water, we also examined the effect of water on the product distribution (Table 4). Separately, H<sub>2</sub>O of 3 vol%, 5 vol% and 10 vol% was added into the reaction system. Under the optimal reaction conditions, the yield of FDCAM was significantly affected as shown in Table 4. A drop from 66% to 46% was determined by HPLC as the volume of water increased from 3% to 10%. When water was as solvent, no effective activity was detected even though there was a 45% conversion of HMF.

**Table 4.** Effects of water on product distribution.<sup>[a]</sup>

Entry	Water [Vol %]	Conversion <sup>[c]</sup> [%]	Yield <sup>[c]</sup> [%]				
			HMFM	FDCDM	FDCMM	FDCA	FDCAM
1	3	92	4	33	31	1	66
2	5	90	9	30	31	1	62
3	10	84	8	19	26	1	46
4 <sup>[b]</sup>	100	45	0	0	0	1	1

[a] Conditions: 1 MPa O<sub>2</sub>, 100 °C, 6 h, 25 mg Co<sub>x</sub>O<sub>y</sub>-N@C-800, and 25 mg K-OMS-2. [b] Reaction performed in water. [c] Determined by HPLC.

### Reusability

In order to apply the catalysts in commercial-scale production, a test of reusability was performed in five consecutive runs (Figure 7). Under identical reaction conditions, results showed a slight efficiency loss in the oxidation of HMF in five continuous runs. A yield of 80% FDCAM was detected at the fifth run. XRD pattern of Co<sub>x</sub>O<sub>y</sub>-N@C and K-OMS-2 as prepared, mixture of Co<sub>x</sub>O<sub>y</sub>-N@C and K-OMS-2 after the fifth run were exhibited in the Figure S5. No significant difference in structure of catalysts between the two states was observed.

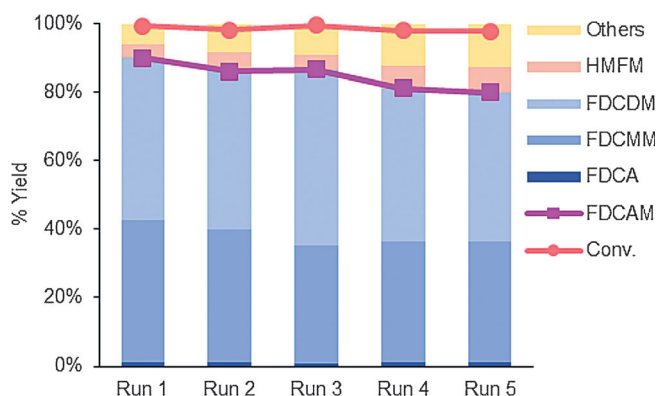


**Figure 7.** Reusability of Co<sub>x</sub>O<sub>y</sub>-N@C catalysts.

## Conclusions

We verified the feasibility of Co<sub>x</sub>O<sub>y</sub>-N@C catalysts applied to the oxidative esterification of HMF and furfural. In addition, full conversion of reactants and high yield of esters were achieved simultaneously. Briefly, we presented a novel, cost-efficient, eco-friendly and recyclable method for the production of FDCAM. The catalyst with the highest activity was prepared using homogeneous cobalt with 1,10-phen as ligand pyrolyzed at 800 °C for 2 h after adsorption on active carbon. The reason can be well-explained by the measurements and data of XPS and TGA. Under the optimal conditions, 1 MPa O<sub>2</sub> at 100 °C for 6 h, we obtained FDCAM in the yield of 96%. Reusability studies were performed with a view to industrial scale production. To our delight, no significant loss of activity was detected up to the fifth run.

## Experimental Section

### Materials

All the chemicals involved in the preparation of catalysts were commercial available. Co(OAc)<sub>2</sub>·4H<sub>2</sub>O and EtOH from SCR, 1,10-phen and 2,2-diPy by Alfa and active carbon from TCI were used as purchased in the preparation of the Co<sub>x</sub>O<sub>y</sub>-N@C catalysts. Materials used in reactions including HMF, FDCA, and FDCDM were generous gifts from Hefei Leaf Energy Biotechnology Co., Ltd. FDCMM was self-made; the detailed preparation process was shown in the Supporting Information. And the left chemicals including HMFM, DFF, methanol, K<sub>2</sub>CO<sub>3</sub>, Na<sub>2</sub>CO<sub>3</sub>, KHCO<sub>3</sub>, NaOAc and Na<sub>2</sub>HPO<sub>4</sub> were commercial available, reagent water was purchased from Wahaha.

### Catalyst preparation

Catalyst Co<sub>x</sub>O<sub>y</sub>-N@C was prepared as demonstrated in the published literature.<sup>[12]</sup> Co(OAc)<sub>2</sub>·4H<sub>2</sub>O (3 mmol) and 1,10-phen (6 mmol) with a molar ratio 1:2 was stirred in 300 mL ethanol for 30 min at room temperature. Then, 4.14 g active carbon was added in for absorption of the products. The reaction system was refluxed at 110 °C for 4 h followed by rotary evaporation at 25 °C. Obtained solid was dried at 60 °C for 12 h in vacuum, and finally pyrolyzed in N<sub>2</sub> (20 mLmin<sup>-1</sup>) at 800 °C (a rate of 10 °Cmin<sup>-1</sup> from

RT to 800 °C) for 2 h. An coupled plasma (ICP) test showed the Co loading in the catalysts was 3.36%.

### Catalytic oxidation of HMF

All the oxidative esterification reactions was performed in the autoclave provided by Anhui Kemi Machinery Technology Co., Ltd. (Figure S9, Supporting Information). Typically, a mixture of 4 mL methanol and 0.5 mmol HMF reacted with the aid of 25 mg  $\text{Co}_x\text{O}_y\text{-N@C}$ , 25 mg K-OMS-2 and 0.1 mmol  $\text{K}_2\text{CO}_3$ .  $\text{O}_2$  was used as the oxidant with a pressure of 1 MPa. Then the reactor was closed, heated to 100 °C and stirred for 6 h. Products were separated by Hitachi L2000 HPLC System, Alltech C18 column at 30 °C at a wavelength of 265 nm. The mobile phase was 30% methanol and 0.1% phosphoric acid aqueous with a rate of 1 mL min<sup>-1</sup>.

### Catalyst characterization

Catalysts were characterized by XRD, TGA, XPS, TEM, ICP, BET surface area analysis, and energy-dispersive X-ray spectroscopy elemental mapping (EDS). Relevant measurements and data are provided in part 3 of the Supporting Information.

### Acknowledgements

This work was supported by the 973 Program (2012CB215305, 2013CB228103), NSFC (21402181, 21325208, 21172209, 21272050), CAS (KJCX2-EW-J02), FRFCU (WK2060190025, WK2060190033), SRFDP (20123402130008) and China Postdoctoral Science Foundation (2014M561835). The authors thank the Hefei Leaf Energy Biotechnology Co., Ltd. and Anhui Kemi Machinery Technology Co., Ltd. for free sample sponsoring in this study.

**Keywords:** 2,5-furandicarboxylic acid dimethyl ester • 5-hydroxymethylfurfural • cobalt oxides • heterogeneous catalysis • oxidative esterification

- [1] a) G. W. Huber, S. Iborra, A. Corma, *Chem. Rev.* **2006**, *106*, 4044–4098; b) J. N. Chheda, G. W. Huber, J. A. Dumesic, *Angew. Chem. Int. Ed.* **2007**, *46*, 7164–7183; *Angew. Chem.* **2007**, *119*, 7298–7318; c) D. R. Dodds, R. A. Gross, *Science* **2007**, *318*, 1250–1251; d) A. Corma, S. Iborra, A. Velty, *Chem. Rev.* **2007**, *107*, 2411–2502; e) J. C. Serrano-Ruiz, J. A. Dumesic, *Energy Environ. Sci.* **2011**, *4*, 83–99; f) Y. Huang, Y. Fu, *Green Chem.* **2013**, *15*, 1095–1111; g) M. Besson, P. Gallezot, C. Pinel, *Chem. Rev.* **2014**, *114*, 1827–1870.
- [2] a) G. Yong, Y. Zhang, J. Y. Ying, *Angew. Chem. Int. Ed.* **2008**, *47*, 9345–9348; *Angew. Chem.* **2008**, *120*, 9485–9488; b) J. B. Binder, R. T. Raines, *J. Am. Chem. Soc.* **2009**, *131*, 1979–1985; c) X. Tong, Y. Ma, Y. Li, *Appl. Catal. A* **2010**, *385*, 1–13; d) A. Corma, O. d. L. Torre, M. Renz, N. Vollandier, *Angew. Chem. Int. Ed.* **2011**, *50*, 2375–2378; *Angew. Chem.* **2011**, *123*, 2423–2426; e) L. Hu, G. Zhao, W. Hao, X. Tang, Y. Sun, L. Lin, S. Liu, *RSC Adv.* **2012**, *2*, 11184–11206; f) R. Van Putten, J. C. V. D. Waal, E. D. Jong, C. B. Rasrendra, H. J. Heeres, J. G. D. Vries, *Chem. Rev.* **2013**, *113*, 1499–1597; g) V. Choudhary, S. H. Mushrif, C. Ho, A. Anderko, V. Nikolakis, N. S. Marinkovic, A. I. Frenkel, S. I. Sandler, D. G. Vlachos, *J. Am. Chem. Soc.* **2013**, *135*, 3997–4006.
- [3] a) A. Gandini, *Macromolecules* **2008**, *41*, 9491–9504; b) A. Gandini, A. Silvestre, C. P. Neto, A. F. Sousa, M. Gomes, *J. Polym. Sci. Part A* **2009**, *47*, 295–298; c) A. Gandini, D. Coelho, M. Gomes, B. Reis, A. Silvestre, *J. Mater. Chem.* **2009**, *19*, 8656–8664; d) M. Gomes, A. Gandini, A. J. D. Silvestre, B. Reis, *J. Polym. Sci. Part A* **2011**, *49*, 3759–3768; e) A. J. J. E. Eerhart, A. P. C. Faaij, M. K. Patel, *Energy Environ. Sci.* **2012**, *5*, 6407–6422; f) J. Ma, X. Yu, J. Xu, Y. Pang, *Polymer* **2012**, *53*, 4145–4151; g) J. Ma, Y. Pang, M. Wang, J. Xu, H. Ma, X. Nie, *J. Mater. Chem.* **2012**, *22*, 3457–3481.
- [4] S. E. Davis, L. R. Houk, E. C. Tamargo, A. K. Datye, R. J. Davis, *Catal. Today* **2011**, *160*, 55–60.
- [5] a) M. A. Lilga, R. T. Hallen, M. Gray, *Top. Catal.* **2010**, *53*, 1264–1269; b) S. E. Davis, B. N. Zope, R. J. Davis, *Green Chem.* **2012**, *14*, 143.
- [6] a) B. Saha, S. Dutta, M. M. Abu-Omar, *Catal. Sci. Technol.* **2012**, *2*, 79–81; b) O. Casanova, S. Iborra, A. Corma, *ChemSusChem* **2009**, *2*, 1138–1144; c) Y. Y. Gorbanev, S. K. Klitgaard, J. M. Woodley, C. H. Christensen, A. Riisager, *ChemSusChem* **2009**, *2*, 672–675; d) J. Cai, H. Ma, J. Zhang, Q. Song, Z. Du, Y. Hu, J. Xu, *Chem. Eur. J.* **2013**, *19*, 14215–14223; e) N. K. Gupta, S. Nishimura, A. Takagaki, K. Ebitani, *Green Chem.* **2011**, *13*, 824; f) G. Yi, S. P. Teong, X. Li, Y. Zhang, *ChemSusChem* **2014**, *7*, 2131–2135; g) S. P. Teong, G. Yi, X. Cao, Y. Zhang, *ChemSusChem* **2014**, *7*, 2120–2124.
- [7] a) T. Ståhlberg, E. Eyjólfsson, Y. Y. Gorbanev, I. Sádaba, *Catal. Lett.* **2012**, *142*, 1089–1097; b) N. Lucas, N. R. Kanna, A. S. Nagpure, G. Kokate, S. Chilukuri, *J. Chem. Sci.* **2014**, *126*, 403–413; c) Y. Y. Gorbanev, S. Kegnaes, A. Riisager, *Catal. Lett.* **2011**, *141*, 1752–1760.
- [8] a) A. Villa, M. Schiavoni, S. Campisi, G. M. Veith, L. Prati, *ChemSusChem* **2013**, *6*, 609–612; b) T. Pasini, M. Piccinini, M. Blosi, R. Bonelli, S. Albonetti, N. Dimitratos, J. A. Lopez-Sanchez, M. Sankar, Q. He, C. J. Kiely, G. J. Hutchings, F. Cavani, *Green Chem.* **2011**, *13*, 2091–2099; c) H. Ait-Rass, N. Essayem, M. Besson, *Green Chem.* **2013**, *15*, 2240–2251.
- [9] M. L. Ribeiro, U. Schuchardt, *Catal. Commun.* **2003**, *4*, 83–86.
- [10] E. Taarning, I. S. Nielsen, K. Egeblad, R. Madsen, C. H. Christensen, *ChemSusChem* **2008**, *1*, 75–78.
- [11] O. Casanova, S. Iborra, A. Corma, *J. Catal.* **2009**, *265*, 109–116.
- [12] a) R. V. Jagadeesh, G. Wienhöfer, F. A. Westerhaus, A. Surkus, M. Pohl, H. Junge, K. Junge, M. Beller, *Chem. Commun.* **2011**, *47*, 10972–10974; b) R. V. Jagadeesh, H. Junge, M. Pohl, J. Radnik, A. Brückner, M. Beller, *J. Am. Chem. Soc.* **2013**, *135*, 10776–10782; c) F. A. Westerhaus, R. V. Jagadeesh, G. Wienhöfer, M. Pohl, J. Radnik, A. Surkus, J. Rabeah, K. Junge, H. Junge, M. Nielsen, A. Brückner, M. Beller, *Nat. Chem.* **2013**, *5*, 537–543; d) R. V. Jagadeesh, A. Surkus, H. Junge, M. Pohl, J. Radnik, J. Rabeah, H. Huan, V. Schünemann, A. Brückner, M. Beller, *Science* **2013**, *342*, 1073–1076; e) D. Banerjee, R. V. Jagadeesh, K. Junge, M. Pohl, J. Radnik, A. Brückner, M. Beller, *Angew. Chem. Int. Ed.* **2014**, *53*, 4359–4363; *Angew. Chem.* **2014**, *126*, 4448–4452.
- [13] G. Liu, X. Li, P. Ganesan, B. N. Popov, *Electrochim. Acta* **2010**, *55*, 2853–2858.
- [14] J. Casanovas, J. M. Ricart, J. Rubio, F. Illas, J. M. Jiménez-Mateos, *J. Am. Chem. Soc.* **1996**, *118*, 8071–8076.
- [15] A. Morozan, P. Jégou, B. Jousselmé, S. Palacin, *Phys. Chem. Chem. Phys.* **2011**, *13*, 21600–21607.
- [16] Z. Yang, J. Deng, T. Pan, Q. Guo, Y. Fu, *Green Chem.* **2012**, *14*, 2986–2989.
- [17] D. Poletti, D. R. Stojaković, *Thermochim. Acta* **1992**, *205*, 225–233.
- [18] a) Y. Ma, H. Zhang, H. Zhong, T. Xu, H. Jin, Y. Tang, Z. Xu, *Electrochim. Acta* **2010**, *55*, 7945–7950; b) Y. Ji, Z. Li, S. Wang, G. Xu, X. Yu, *Int. J. Hydrogen Energy* **2010**, *35*, 8117–8121.
- [19] a) C. W. B. Bezerra, L. Zhang, K. Lee, *Electrochim. Acta* **2008**, *53*, 7703–7710; b) S. Li, L. Zhang, H. Liu, *Electrochim. Acta* **2010**, *55*, 4403–4411.
- [20] a) X. Li, G. Liu, B. N. Popov, *J. Power Sources* **2010**, *195*, 6373–6378; b) U. Koslowski, I. Herrmann, P. Bogdanoff, *ECS Trans.* **2008**, *13*, 125–141.
- [21] M. Bron, S. Fiechter, M. Hilgendorff, *J. Appl. Electrochem.* **2002**, *32*, 211–216.
- [22] a) L. Zhang, K. Lee, C. W. B. Bezerra, *Electrochim. Acta* **2009**, *54*, 6631–6636; b) M. Lefèvre, J. P. Dodelet, P. Bertrand, *J. Phys. Chem.* **2000**, *104*, 11238–11247.

Received: August 17, 2014

Revised: August 28, 2014

Published online on ■■■■■, 0000

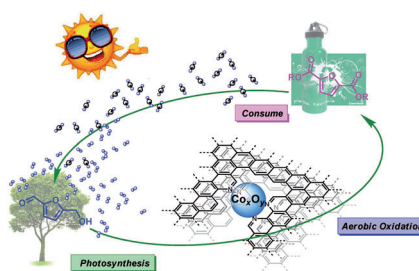
## FULL PAPERS

J. Deng, H.-J. Song, M.-S. Cui, Y.-P. Du,  
Y. Fu\*

■■■ – ■■■



**Aerobic Oxidation of  
Hydroxymethylfurfural and Furfural  
by Using Heterogeneous  $\text{Co}_x\text{O}_y\text{-N@C}$   
Catalysts**



**Happy Ester:** The oxidative esterification of 5-hydroxymethylfurfural (HMF) and furfural over  $\text{Co}_x\text{O}_y\text{-N@C}$  catalysts is performed using  $\text{O}_2$  as benign oxidant, obtaining the corresponding esters. High yield and selectivity of 2,5-furandicarboxylic acid methyl and methyl 2-furoate are achieved under optimized conditions.



